IMA Journal of Numerical Analysis (2019) **00**, 1–22
doi:10.1093/imanum/drz028

Downloaded from https://academic.oup.com/imajna/advance-article-abstract/doi/10.1093/imanum/drz028/5526934 by University of Edinburgh user on 08 December 2019

The inf-sup stability of the lowest order Taylor–Hood pair on affine anisotropic meshes

Gabriel R. Barrenechea
Department of Mathematics and Statistics, University of Strathclyde, 26 Richmond Street, Glasgow G1 1XH, UK
Email: gabriel.barrenechea@strath.ac.uk

and

Andreas Wachtel*
Department of Mathematics, Instituto Tecnológico Autónomo de México, Río Hondo 1, Ciudad de México 01080, Mexico
*Corresponding author: andreas.wachtel@itam.mx

[Received on 19 April 2018; revised on 4 February 2019]

Uniform inf-sup conditions are of fundamental importance for the finite element solution of problems in incompressible fluid mechanics, such as the Stokes and Navier–Stokes equations. In this work we prove a uniform inf-sup condition for the lowest-order Taylor–Hood pairs $\mathbb{Q}_2 \times \mathbb{Q}_1$ and $\mathbb{P}_2 \times \mathbb{P}_1$ on a family of affine anisotropic meshes. These meshes may contain refined edge and corner patches. We identify necessary hypotheses for edge patches to allow uniform stability and sufficient conditions for corner patches. For the proof, we generalize Verfürth's trick and recent results by some of the authors. Numerical evidence confirms the theoretical results.

Keywords: anisotropic mesh; Taylor; Hood; inf-sup condition.

1. Introduction

The finite element method for the Stokes problem is subject to the satisfaction of the discrete inf-sup condition. For an effective method the discrete velocity and pressure spaces should be balanced correctly. This balance results in a discrete inf-sup constant which is independent of mesh properties, such as the size and shape of the elements. Concerning the first requirement, there are many finite element pairs that have been proved to be inf-sup stable on regular meshes (see Boffi *et al.*, 2013 for an extensive review). Concerning the second requirement, for the vast majority of methods the discrete inf-sup constant has only been proved to be independent of the size of the elements but may depend on the aspect ratio of the elements of the partition.

This work addresses the last point raised in the previous paragraph. The stability of finite element pairs has been less studied in the anisotropic case, but some progress has been made for some specific pairs, especially using discontinuous pressures and, possibly, nonconforming elements for the velocity. For example, in the work of Durán & Lombardi (2008) the authors analyze the Raviart–Thomas element of arbitrary order on triangular and tetrahedral meshes under a maximum angle condition. Another example is Apel *et al.* (2001) where the authors analyze the Crouzeix–Raviart element in anisotropic meshes (see also Acosta & Durán, 1999). In Schötzau & Schwab (1998) and Schötzau *et al.* (1999) the authors consider quadrilateral and triangular elements for the *hp*-FEM and analyze pairs like

© The Author(s) 2019. Published by Oxford University Press on behalf of the Institute of Mathematics and its Applications. All rights reserved.

$\mathbb{Q}^2_{k+1} \times \mathbb{Q}_{k-1}$ ($k \geq 1$) with continuous velocities and discontinuous pressures. Their analysis shows that this family is uniformly inf-sup stable in edge patches, but corner patches were excluded. This is later analytically justified in Ainsworth & Coggins (2000), where the quadrilateral element $\mathbb{Q}^2_{k+1} \times \mathbb{P}_{k-1}$ was analyzed and it was proved that its inf-sup constant depends on the geometric properties of the quadrilaterals in corner patches. In the same reference the authors propose an enrichment of the velocity space with bubble functions whose degree depends on the aspect ratio. Alternatively, in the recent work Ainsworth *et al.* (2015) a penalization based on jumps of the pressure was designed to show inf-sup stability independent of the aspect ratio of the partition. For a review and further references on this topic see Apel & Randrianarivony (2003).

In this work we study the stability of the lowest-order Taylor–Hood pair on a family of affine anisotropic meshes. This pair was originally proposed in Taylor & Hood (1973) and was first analyzed in Bercovier & Pironneau (1979) and Verfürth (1984) for the lowest order on triangles. In the independent works Brezzi & Falk (1991) and Stenberg (1990) the analysis was extended to higher-order families, both in the triangular and quadrilateral cases, in two space dimensions. Later, in Boffi (1994, 1997), the general two- and three-dimensional triangular and tetrahedral cases were addressed. As is well known (see, e.g., Girault & Raviart, 1986, Lemma 1.1), the validity of the inf-sup condition is equivalent to the existence of a Fortin operator. In Falk (2008) an explicit construction of this operator is presented for the quadratic and cubic cases. In Mardal *et al.* (2013) another explicit construction was built for the lowest-order two-dimensional case, and the result was used to justify a preconditioner for a singularly perturbed problem on shape-regular meshes. Some aspects of this explicit construction were later simplified in Chen (2014).

As far as we are aware, no general proof of stability is available for the Taylor–Hood pair in the anisotropic case, and only very particular cases have been analyzed so far. For instance, the result Braack *et al.* (2012, Lemma 3.1) states an explicit dependency on the aspect ratio, under the assumption that no drastic changes of size of neighboring cells in any direction may occur; see Braack *et al.* (2012, Assumption 1). Moreover, for some anisotropic edge patches, negative results, in the form of numerical experiments, are given in Schötzau *et al.* (1999) and Apel & Randrianarivony (2003). In particular, in Apel & Randrianarivony (2003) instabilities are reported for the $\mathbb{P}^2_2 \times \mathbb{P}_1$ pair when the aspect ratio tends to zero in certain configurations. These numerical results (and some results presented in the present work) show that a proof of the uniform stability of the Taylor–Hood pair on general anisotropic meshes cannot be given.

Based on the above discussions the purpose of this paper is to present a proof for a family of affine anisotropic meshes containing patches of parallelograms and triangular meshes appearing as a result of dividing each parallelogram into two triangles. The results presented below are valid for edge and corner patches (thus improving upon the results from Braack *et al.*, 2012), but they do not cover the case in which the mesh does not have a structure. In particular, our results do not include the case of general quadrilaterals or when the elements cannot be arranged into corner or edge patches. Our main results state that if the partitions have enough internal degrees of freedom (dof), and these are at the right locations, then this element is uniformly inf-sup stable. That is, the inf-sup constant is independent of the aspect ratio and drastic changes of size. Finally, we will show by means of numerical experiments that our assumptions are optimal, which complements the results from Apel & Randrianarivony (2003).

The rest of the paper is organized as follows. In Section 2 we present the problem of interest and give some notation. Our main results are then stated in Section 3 and tested numerically in Section 4. The proofs for the quadrilateral case are then presented in Section 5 and for the triangular case in Section 6.

Downloaded from https://academic.oup.com/imajna/advance-article-abstract/doi/10.1093/imanum/drz028/5526934 by University of Edinburgh user on 08 December 2019

2. Preliminaries and notation

Let $\Omega \subset \mathbb{R}^2$ be an open, bounded, connected and polygonal domain. Throughout we use standard notation for Sobolev spaces (see Girault & Raviart, 1986); namely, for $D \subset \Omega$, $L^2(D)$ (resp., $L^2_0(D)$) stands for the space of (generalized) functions that are square integrable in D (resp., which belong to $L^2(D)$ and have zero mean value in D); $H^1(D)$ ($H^1_0(D)$) are elements of $L^2(D)$ whose first-order derivatives belong to $L^2(D)$ (and whose trace is zero on ∂D). Vector-valued spaces and functions will be denoted using bold-faced letters. The inner product in $L^2(D)$ (or $\boldsymbol{L}^2(D)$) is denoted by $(\cdot,\cdot)_D$, with associated norm $\|\cdot\|_{0,D}$; the norm (seminorm) in $H^1(D)$ is denoted by $\|\cdot\|_{1,D}$ ($|\cdot|_{1,D}$). By virtue of the Poincaré inequality $|\cdot|_{1,D}$ is a norm on $H^1_0(D)$. Finally, we denote by χ_D the characteristic function of D.

A classical result (see Girault & Raviart, 1986) is the following inf-sup condition: there exists $\beta_\Omega > 0$, depending only on Ω, such that

$$\inf_{q\in M}\sup_{\boldsymbol{v}\in \boldsymbol{V}} \frac{(\operatorname{div}\boldsymbol{v}, q)_\Omega}{|\boldsymbol{v}|_{1,\Omega}\,\|q\|_{0,\Omega}} \geq \beta_\Omega > 0, \tag{2.1}$$

where $\boldsymbol{V}\times M := \boldsymbol{H}^1_0(\Omega)\times L^2_0(\Omega)$. The purpose of this work is to prove the discrete analogue of this result for the lowest-order Taylor–Hood element on a family of anisotropic meshes defined in the next section.

2.1 *Restrictions on partitions*

We require a partition $\mathcal{P}$ of Ω to have the following properties. We suppose Ξ is a conforming shape-regular partition of Ω into parallelograms (macro elements). These macro-element cells are denoted by ω. The partition $\mathcal{P}$ is a conforming refinement of Ξ and may contain edge patches as in Fig. 1(d–f) and corner patches as in Fig. 2(c, d) (for rectangular patches), or affine images of these, as depicted in Fig. 4. Our proof is rigorous for such meshes and the Taylor–Hood pair on their triangulated versions; that is, each parallelogram is divided into two triangles of equal area; see Section 6.

Concerning further refined edge patches, in Remark 3.3 we conjecture that a similar proof is valid. We refer to Remark 3.3 and the numerical evidence for more details.

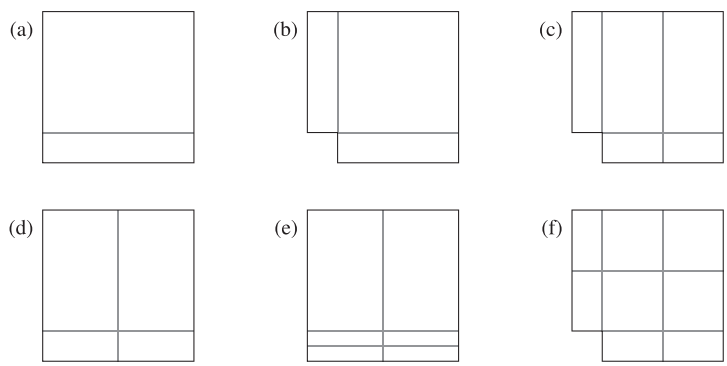

FIG. 1. Edge patches. The cases in the top row do not satisfy Hypothesis 3.1, but the cases in the bottom row do satisfy it. The examples depicted in (b), (c) and (f) are overlapped edge patches.

Downloaded from https://academic.oup.com/imajna/advance-article-abstract/doi/10.1093/imanum/drz028/5526934 by University of Edinburgh user on 08 December 2019

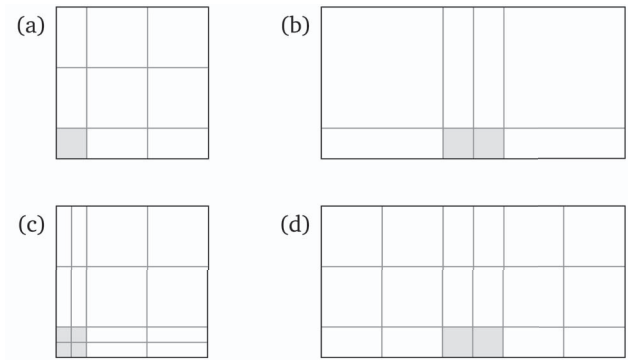

FIG. 2. Corner patches. Case (a) does not satisfy Hypothesis 3.4, the others do. However, the assumptions of Theorem 3.5 also exclude case (b) since the 'overlapped' edge patch does not satisfy Hypothesis 3.1.

2.2 *Finite element spaces*

We now define the discontinuous space

$$\mathbb{Q}_{-\ell,\mathcal{P}} := \left\{ q \in L^2(\Omega) : \ q|_K \in \mathbb{Q}_\ell(K) \text{ for } K \in \mathcal{P} \right\} \quad \text{for} \quad \ell = 1, 2,$$

and for $\omega \subseteq \Omega$ the (locally) continuous spaces

$$\mathbb{Q}_{\ell,\mathcal{P}}(\omega) := \left\{ q \in \mathbb{Q}_{-\ell,\mathcal{P}} : \operatorname{supp} q \subseteq \overline{\omega} \right\} \cap C^0(\omega).$$

Let $M_{\mathcal{P}}(\omega) := \mathbb{Q}_{1,\mathcal{P}}(\omega) \cap L^2_0(\omega)$; in the case of $\omega = \Omega$ we write $M_{\mathcal{P}}$ for short. Let $\boldsymbol{V}_{\mathcal{P}}(\omega) := [\mathbb{Q}_{2,\mathcal{P}}(\omega)]^2 \cap \boldsymbol{H}^1_0(\omega)$; in the case of $\omega = \Omega$ we write shortly $\boldsymbol{V}_{\mathcal{P}}$ for short.

Throughout this manuscript, C (with or without subscript) will denote a positive constant, which will be independent of the size and aspect ratio of the elements of a given partition. The value of such a constant need not to be equal whenever written in two different places.

3. Main results

In this section we state the main results of this work. We restrict the presentation to inf-sup conditions on anisotropically partitioned macro elements $\omega \in \Xi$. Since, given such local inf-sup conditions and the shape-regularity of Ξ, a macro-element technique ensures uniform stability on the whole partition $\mathcal{P}$.

To ease the readability the proofs of Theorems 3.2 and 3.5, dealing with rectangular edge and corner patches, respectively, are postponed to Section 5. The proof of the extension of these results to the parallelogram case is given in Theorem 3.7. Finally, we sketch in Section 6 how the proofs can be extended to triangulated edge and corner patches. Before stating the results we state the main hypothesis for edge patches.

HYPOTHESIS 3.1 We will suppose that every edge patch contains at least one division in the direction orthogonal to the 'long and thin' elements. More precisely, every 'long and thin' element is divided into two 'shorter' elements.

Downloaded from https://academic.oup.com/imajna/advance-article-abstract/doi/10.1093/imanum/drz028/5526934 by University of Edinburgh user on 08 December 2019

THEOREM 3.2 Let $\omega \subset \Omega$ be partitioned as an edge patch as depicted in Fig. 1(d–f). Then there exists a constant $\beta > 0$, independent of the shape and size of the elements in $\mathcal{P}$, such that

$$\inf_{q \in M_{\mathcal{P}}(\omega)} \sup_{\boldsymbol{v} \in \boldsymbol{V}_{\mathcal{P}}(\omega)} \frac{(\operatorname{div} \boldsymbol{v}, q)_{\omega}}{|\boldsymbol{v}|_{1,\omega} \, \|q\|_{0,\omega}} \geq \beta. \tag{3.1}$$

REMARK 3.3 One clear consequence of the proof of Theorem 3.2 is that the inf-sup constant β is the same one for the cases depicted in Fig. 1(d,e). This opens the door to study the case in which an edge patch has been refined further. More precisely, if we say that the edge patch in Fig. 1(d) is refined $r = 0$ times, and the patch in Fig. 1(e) is refined $r = 1$ times, then, continuing in the same way, that is, bisecting the long and thin elements r times, we can define a patch that has been refined $r \geq 2$ times, for example, Fig. 5. Our conjecture, which is supported by numerical evidence shown in Table 4, is that the inf-sup constant (on edge patches) is not affected by the value of r, but a formal proof of this fact is lacking.

The next result concerns corner patches. A corner patch will be decomposed as $\omega = \omega_{\boldsymbol{c}} \cup \omega_E$ where $\omega_{\boldsymbol{c}}$ is the shape-regular small region (shaded in Fig. 2 for each corner patch) and ω_E is an 'overlapped' edge patch as discussed in Theorem 3.2 (Fig. 1). For the proof of Theorem 3.5 we will need the following assumption.

HYPOTHESIS 3.4 The partition on $\omega_{\boldsymbol{c}} \subset \omega$ is such that the pair $\boldsymbol{V}_{\mathcal{P}}(\omega_{\boldsymbol{c}}) \times M_{\mathcal{P}}(\omega_{\boldsymbol{c}})$ is (uniformly) inf-sup stable with a constant $\beta_{\boldsymbol{c}}$.

THEOREM 3.5 Let $\omega \subset \Omega$ be partitioned into a corner patch, that is, $\omega = \omega_{\boldsymbol{c}} \cup \omega_E$ with $\omega_{\boldsymbol{c}}$ and ω_E satisfying Hypothesis 3.1 and Theorem 3.2, respectively (e.g., as shown in Fig. 2 (c,d)). Then there exists $\beta_{\mathcal{P}} > 0$, depending only on β (from (3.1)) and $\beta_{\boldsymbol{c}}$ (from Hypothesis 3.4), such that

$$\inf_{q \in M_{\mathcal{P}}(\omega)} \sup_{\boldsymbol{v} \in \boldsymbol{V}_{\mathcal{P}}(\omega)} \frac{(\operatorname{div} \boldsymbol{v}, q)_{\omega}}{|\boldsymbol{v}|_{1,\omega} \, \|q\|_{0,\omega}} \geq \beta_{\mathcal{P}}.$$

REMARK 3.6 A comment on Hypothesis 3.1 is in order. In the case of a single corner patch, Hypothesis 3.1 requires $\omega_{\boldsymbol{c}}$ to be refined (as in Fig. 2(c)). Now, if a corner patch is formed by 'joining' several patches of the type shown in Fig. 2(a), see for instance Fig. 2(d), then the presence of enough dof inside $\omega_{\boldsymbol{c}}$ ensures that Hypothesis 3.1 is satisfied without the need of further refinement.

The results presented in Theorems 3.2 and 3.5 remain valid on affine images of allowed edge and corner patches and meshes that contain such; see for instance the examples in Fig. 4. The next result shows such an extension.

THEOREM 3.7 Let $\hat{\omega}$ be a rectangular edge or corner patch that satisfies the hypotheses of Theorems 3.2 or 3.5, and let $\omega \in \Xi$ be the image of $\hat{\omega}$ under a bijective affine map $\mathcal{F}_{\omega} : \hat{\omega} \to \omega$. Then there exists a constant $\beta_{\mathcal{A}}$, depending only on the shape of ω, such that

$$\inf_{q \in M_{\mathcal{P}}(\omega)} \sup_{\boldsymbol{v} \in \boldsymbol{V}_{\mathcal{P}}(\omega)} \frac{(\operatorname{div} \boldsymbol{v}, q)_{\omega}}{|\boldsymbol{v}|_{1,\omega} \, \|q\|_{0,\omega}} \geq \beta_{\mathcal{A}}\,.$$

Proof. Let $\mathcal{F}_{\omega}(\hat{\boldsymbol{x}}) = \mathbb{A}\hat{\boldsymbol{x}} + \boldsymbol{b}$, and let us denote $J := \det(\mathbb{A}) \neq 0$. Let, for $\hat{\boldsymbol{v}} \in H^1(\hat{\omega})^2$, $\boldsymbol{v} \in H^1(\omega)^2$ be its Piola transorm given by

$$\boldsymbol{v}(\boldsymbol{x}) := |J|^{-1} \mathbb{A}\hat{\boldsymbol{v}}(\hat{\boldsymbol{x}}) \quad \text{where} \quad \boldsymbol{x} = \mathcal{F}_{\omega}(\hat{\boldsymbol{x}}). \tag{3.2}$$

Downloaded from https://academic.oup.com/imajna/advance-article-abstract/doi/10.1093/imanum/drz028/5526934 by University of Edinburgh user on 08 December 2019

It is well known (see, e.g., Durán, 2008, Lemma 3.3) that

$$(\operatorname{div} \boldsymbol{v}, q)_\omega = \left(\widehat{\operatorname{div}}\, \hat{\boldsymbol{v}}, \hat{q}\right)_{\hat{\omega}} \tag{3.3}$$

for all $\boldsymbol{v} \in H^1(\omega)^2$ and all $q \in H^1(\omega)$. Here we have denoted $\hat{q}(\hat{\boldsymbol{x}}) \coloneqq q(\mathcal{F}_\omega(\hat{\boldsymbol{x}})) = q(\boldsymbol{x})$ and by $\widehat{\operatorname{div}}$ the divergence with respect to the variable $\hat{\boldsymbol{x}}$. This notation will be extended to any derivatives later on. Next the chain rule gives

$$\nabla \boldsymbol{v}(\boldsymbol{x}) = |J|^{-1} \mathbb{A} \nabla (\hat{\boldsymbol{v}} \circ \mathcal{F}_\omega^{-1})(\boldsymbol{x}) = |J|^{-1} \mathbb{A} \widehat{\nabla} \hat{\boldsymbol{v}}(\hat{\boldsymbol{x}}) \mathbb{A}^{-1},$$

and then, using the shape-regularity of ω and $\hat{\omega}$ (to bound the norms of $\mathbb{A}$ and $\mathbb{A}^{-1}$) and changing variables we obtain

$$\begin{aligned}
|\boldsymbol{v}|_{1,\omega}^2 &= \int_\omega |\nabla \boldsymbol{v}(\boldsymbol{x})|^2 \, \mathrm{d}\boldsymbol{x} \\
&= \int_\omega |J|^{-2} |\mathbb{A} \widehat{\nabla} \hat{\boldsymbol{v}}(\hat{\boldsymbol{x}}) \mathbb{A}^{-1}|^2 \, \mathrm{d}\boldsymbol{x} \\
&\leq C |J|^{-2} \int_\omega \|\mathbb{A}\|_2^2 |\widehat{\nabla} \hat{\boldsymbol{v}}(\hat{\boldsymbol{x}})|^2 \|\mathbb{A}^{-1}\|_2^2 \, \mathrm{d}\boldsymbol{x} \\
&\leq C_0 |J|^{-2} \int_\omega |\widehat{\nabla} \hat{\boldsymbol{v}}(\hat{\boldsymbol{x}})|^2 \, \mathrm{d}\boldsymbol{x} \\
&= C_0 |J|^{-1} |\hat{\boldsymbol{v}}|_{1,\hat{\omega}}^2,
\end{aligned} \tag{3.4}$$

where the constant C_0 depends only on the shape of ω. In addition, a change of variables gives

$$\|q\|_{0,\omega} = |J|^{\frac{1}{2}} \|\hat{q}\|_{0,\hat{\omega}}. \tag{3.5}$$

Finally, from Theorems 3.2 and 3.5 (depending whether $\hat{\omega}$ is decomposed into an edge or a corner patch, respectively), there exists a constant $\hat{\beta} > 0$ such that for all $\hat{q} \in M_{\mathcal{P}}(\hat{\omega})$ the following holds:

$$\hat{\beta} \|\hat{q}\|_{0,\tilde{\omega}} \leq \sup_{\hat{\boldsymbol{v}} \in \boldsymbol{V}_{\mathcal{P}}(\hat{\omega})} \frac{\left(\widehat{\operatorname{div}}\, \hat{\boldsymbol{v}}, \hat{q}\right)_{\hat{\omega}}}{|\hat{\boldsymbol{v}}|_{1,\hat{\omega}}}. \tag{3.6}$$

Hence, using (3.5), (3.6), (3.3) and (3.4) we obtain for all $q \in M_{\mathcal{P}}(\omega)$,

$$\begin{aligned}
\hat{\beta} \|q\|_{0,\omega} &= \hat{\beta} |J|^{\frac{1}{2}} \|\hat{q}\|_{0,\hat{\omega}} \\
&\leq |J|^{\frac{1}{2}} \sup_{\hat{\boldsymbol{v}} \in \boldsymbol{V}_{\mathcal{P}}(\hat{\omega})} \frac{\left(\widehat{\operatorname{div}}\, \hat{\boldsymbol{v}}, \hat{q}\right)_{\hat{\omega}}}{|\hat{\boldsymbol{v}}|_{1,\hat{\omega}}} \\
&= |J|^{\frac{1}{2}} \sup_{\boldsymbol{v} \in \boldsymbol{V}_{\mathcal{P}}(\omega)} \frac{(\operatorname{div} \boldsymbol{v}, q)_\omega}{|\hat{\boldsymbol{v}}|_{1,\hat{\omega}}} \\
&\leq |J|^{\frac{1}{2}} \sup_{\boldsymbol{v} \in \boldsymbol{V}_{\mathcal{P}}(\omega)} \frac{(\operatorname{div} \boldsymbol{v}, q)_\omega}{C_0^{-1} |J|^{\frac{1}{2}} |\boldsymbol{v}|_{1,\omega}},
\end{aligned}$$

and the result follows with $\beta_{\mathcal{A}} \coloneqq \hat{\beta} C_0^{-1}$. □

Downloaded from https://academic.oup.com/imajna/advance-article-abstract/doi/10.1093/imanum/drz028/5526934 by University of Edinburgh user on 08 December 2019

Downloaded from https://academic.oup.com/imajna/advance-article-abstract/doi/10.1093/imanum/drz028/5526934 by University of Edinburgh user on 08 December 2019

4. Numerical confirmation

In this section we report the discrete inf-sup constants for the Taylor–Hood pairs in different configurations of edge and corner patches. Our aim is to confirm the validity of the results from the last section. Then we introduce the parameter h in such a way that the short side of an anisotropic element is of size h, and the long one is $\mathcal{O}(1)$ (see Fig. 3 for details). For the refinement in the direction orthogonal to the long and thin elements required by Hypothesis 3.1, we have introduced an extra edge at the midpoint of the long and thin edges (e.g., in Fig. 1(e) the extra vertical edge is located at $x = 1/2$ and in Fig. 1(f) at $x, y = (1 + h)/2$).

4.1 *Results on edge patches*

Our first experiments (in Table 1) aim to show that Hypothesis 3.1 imposes sufficient (and necessary) requirements on edge patches such that the pair $\mathbb{Q}_2^2 \times \mathbb{Q}_1$ is uniformly stable on them. The results reported in the last two columns of Table 1 show that, once the requirements from Hypothesis 3.1 are fulfilled, the inf-sup constant remains bounded below by a constant independent of h. Now, to assess the necessity of this restriction, we also report in the first two columns of Table 1 the results for partitions that do not satisfy this hypothesis, where we see that the inf-sup constants degenerate with h.

4.2 *Results on corner patches*

In Table 2 we report the results obtained for different configurations of corner patches. We confirm the results of Theorem 3.5 in the sense that whenever the hypotheses imposed on the partitions are satisfied, the inf-sup constant remains bounded below by a constant independent of h (as can be seen in the last two columns). On the contrary, the first column of Table 2 shows that if the hypotheses are violated then the inf-sup constant decays with h.

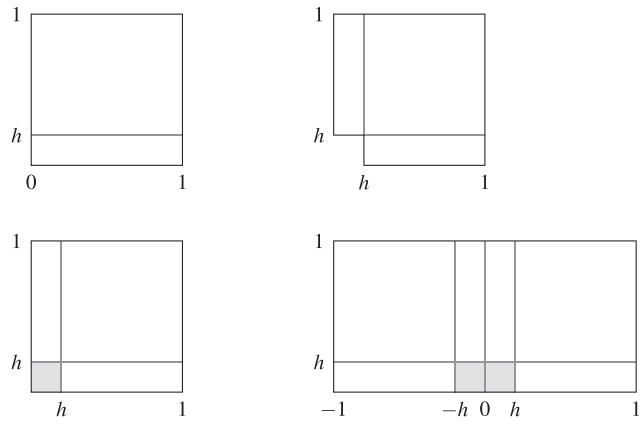

FIG. 3. Parametrized geometries for the coarse partitions of the edge and corner patches shown in Figs 1 and 2. That is, before subdividing cells so that Hypotheses 3.1 and 3.4 are satisfied.

TABLE 1 *Discrete inf-sup constants of the pair $\mathbb{Q}_2^2 \times \mathbb{Q}_1$ on edge patches shown in Fig. 1*

h	Fig. 1(a)	Fig. 1(c)	Fig. 1(d)	Fig. 1(f)
10^{-1}	$7.12 \cdot 10^{-2}$	$1.07 \cdot 10^{-1}$	0.426	0.487
10^{-2}	$7.83 \cdot 10^{-3}$	$1.17 \cdot 10^{-2}$	0.256	0.477
10^{-3}	$7.90 \cdot 10^{-4}$	$1.20 \cdot 10^{-3}$	0.208	0.469
10^{-4}	$7.90 \cdot 10^{-5}$	$1.21 \cdot 10^{-4}$	0.202	0.468
10^{-5}	$7.91 \cdot 10^{-6}$	$1.21 \cdot 10^{-5}$	0.201	0.468

TABLE 2 *Discrete inf-sup constants of the pair $\mathbb{Q}_2^2 \times \mathbb{Q}_1$ on corner patches shown in Fig. 2*

h	Fig. 2(b)	Fig. 2(c)	Fig. 2(d)
10^{-1}	$4.01 \cdot 10^{-1}$	0.455	0.341
10^{-2}	$1.82 \cdot 10^{-1}$	0.406	0.324
10^{-3}	$6.07 \cdot 10^{-2}$	0.384	0.323
10^{-4}	$1.93 \cdot 10^{-2}$	0.382	0.322
10^{-5}	$6.11 \cdot 10^{-3}$	0.381	0.322

4.3 *The stability on affine meshes*

The previous examples were restricted to one single edge, or corner, patch. Next we show two examples in which edge and corner patches are combined. For this, Fig. 4 shows an affine L-shaped mesh (left) and a snowflake mesh (right). To obtain the left mesh we took an L-shaped mesh on $[-2,1] \times [0,1] \cup [0,1] \times [-1,0]$ and applied the map $F(\boldsymbol{x}) := \left(\begin{smallmatrix} 1 & 0 \\ 0.25 & 1 \end{smallmatrix}\right)\boldsymbol{x}$ to all nodes in $[-2,0] \times [0,1]$ and the map $F(\boldsymbol{x}) := \left(\begin{smallmatrix} 1 & 0.5 \\ 0 & 1 \end{smallmatrix}\right)\boldsymbol{x}$ to all nodes in $[0,1] \times [-1,0]$. The snowflake mesh is the union of five corner patches with a minimal angle of 72°; its reentrant corners have a distance of 1 from the origin. Both meshes have in common that the small edges connected to the origin are of length h. Table 3 shows that, once again, the inf-sup constants stay bounded below by a constant independent of the value h, as predicted by Theorem 3.7.

4.4 *Refined patches*

In this section we verify numerically the claims made in Remark 3.3. For this we consider the refined edge and corner patches depicted in Fig. 5. In Table 4 we report the values of the inf-sup constants. We observe that, as was conjectured in Remark 3.3, for the case of a refined edge patch the inf-sup constants reported in the first two columns remain independent of the number of refinements, thus confirming that conjecture, at least numerically. Now, for the case of a refined corner patch, we see that, as mentioned in Remark 5.7 the values of the inf-sup constants (reported in the third column of Table 4) decrease with the number of refinements, thus confirming the sharpness of the proof of Theorem 3.5.

5. Proofs on rectangular meshes

We start with a preliminary result. This slight generalization of John (2016, Theorem 3.89) will be the main tool we will base our proof of stability on.

Downloaded from https://academic.oup.com/imajna/advance-article-abstract/doi/10.1093/imanum/drz028/5526934 by University of Edinburgh user on 08 December 2019

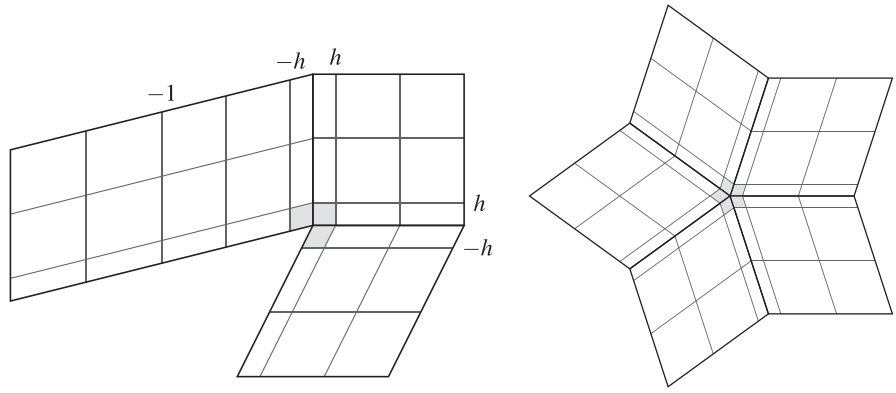

FIG. 4. Meshes with affine corner and edge patches.

TABLE 3 *Inf-sup constants $\beta_{\mathcal{P}}$ of the $\mathbb{Q}_2^2 \times \mathbb{Q}_1$ pair on affine meshes*

h	Fig. 4 (left)	Fig. 4 (right)
10^{-1}	0.21474	0.39513
10^{-2}	0.21242	0.39630
10^{-3}	0.21135	0.39632
10^{-4}	0.21119	0.39632
10^{-5}	0.21118	0.39632
10^{-6}	0.21113	0.39632

LEMMA 5.1 Let us suppose there exists a space $B \subset L^2(\Omega)$, such that

$$\sup_{\boldsymbol{v} \in \boldsymbol{V}_{\mathcal{P}}} \frac{(q, \operatorname{div} \boldsymbol{v})_{\Omega}}{|\boldsymbol{v}|_{1,\Omega}} \geq \beta_1 \|q\|_{0,\Omega} \quad \text{for all } q \in B, \tag{5.1}$$

and a projection $\Pi_B \colon M_{\mathcal{P}} \to B$ such that

$$\sup_{\boldsymbol{v} \in \boldsymbol{V}_{\mathcal{P}}} \frac{(q, \operatorname{div} \boldsymbol{v})_{\Omega}}{|\boldsymbol{v}|_{1,\Omega}} \geq \beta_2 \left\|q - \Pi_B q\right\|_{0,\Omega} \quad \text{for all } q \in M_{\mathcal{P}}, \tag{5.2}$$

where β_1 and β_2 are positive constants. Then $\boldsymbol{V}_{\mathcal{P}} \times M_{\mathcal{P}}$ is inf-sup stable with inf-sup constant $\beta_0 \coloneqq \frac{\beta_1 \beta_2}{1+\beta_1+\beta_2}$, that is,

$$\sup_{\boldsymbol{v} \in \boldsymbol{V}_{\mathcal{P}}} \frac{(q, \operatorname{div} \boldsymbol{v})_{\Omega}}{|\boldsymbol{v}|_{1,\Omega}} \geq \beta_0 \|q\|_{0,\Omega} \quad \text{for all } q \in M_{\mathcal{P}}.$$

Downloaded from https://academic.oup.com/imajna/advance-article-abstract/doi/10.1093/imanum/drz028/5526934 by University of Edinburgh user on 08 December 2019

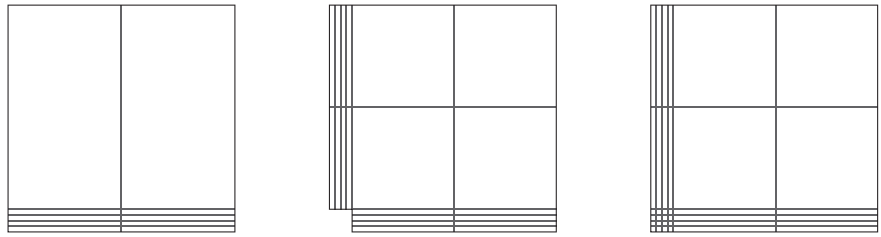

FIG. 5. These patches are refinements of level $r = 2$ of edge patches and a corner patch.

TABLE 4 *We fix the parameter $h = 10^{-3}$. The columns below contain the inf-sup constants on (r-times) refined patches*

r	Fig. 5 (left)	Fig. 5 (center)	Fig. 5 (right)
1	0.2075	0.4693	0.3843
2	0.2075	0.4693	0.3205
3	0.2075	0.4693	0.2503
4	0.2075	0.4693	0.1919

Proof. Let $q \in M_{\mathcal{P}}$. Then using (5.1) we get

$$\sup_{\boldsymbol{v}\in\boldsymbol{V}_{\mathcal{P}}} \frac{(q, \operatorname{div} \boldsymbol{v})_{\Omega}}{|\boldsymbol{v}|_{1,\Omega}} = \sup_{\boldsymbol{v}\in\boldsymbol{V}_{\mathcal{P}}} \left\{ \frac{(\Pi_B q, \operatorname{div} \boldsymbol{v})_{\Omega}}{|\boldsymbol{v}|_{1,\Omega}} + \frac{(q - \Pi_B q, \operatorname{div} \boldsymbol{v})_{\Omega}}{|\boldsymbol{v}|_{1,\Omega}} \right\}$$
$$\geq \beta_1 \left\| \Pi_B q \right\|_{0,\Omega} - \left\| q - \Pi_B q \right\|_{0,\Omega}.$$

Multiplying (5.2) by $(\beta_1 + 1)/\beta_2$ and adding it to the last inequality yields

$$\left(1 + \frac{\beta_1 + 1}{\beta_2}\right) \sup_{\boldsymbol{v}\in\boldsymbol{V}_{\mathcal{P}}} \frac{(q, \operatorname{div} \boldsymbol{v})_{\Omega}}{|\boldsymbol{v}|_{1,\Omega}} \geq \beta_1 \left(\left\| \Pi_B q \right\|_{0,\Omega} + \left\| q - \Pi_B q \right\|_{0,\Omega} \right) \geq \beta_1 \left\| q \right\|_{0,\Omega},$$

as required. □

5.1 Proof of Theorems 3.2

Our aim is to prove the assumptions of Lemma 5.1. For simplicity of the presentation we will consider a local coordinate system and will consider $\omega = [-H, H] \times [-h, h + 2H]$ to be partitioned into an edge patch as shown in Fig. 6. We will consider $\omega = M \cup M'$, where the 'bottom' $M = [-H, H] \times [-h, h]$ is divided into two anisotropic elements, as depicted in Fig. 7 (left), or four anisotropic elements, as in Fig. 7 (right). On the other hand, the 'top' $M' = [-H, H] \times [h, h+2H]$ is divided into two shape-regular elements.

Downloaded from https://academic.oup.com/imajna/advance-article-abstract/doi/10.1093/imanum/drz028/5526934 by University of Edinburgh user on 08 December 2019

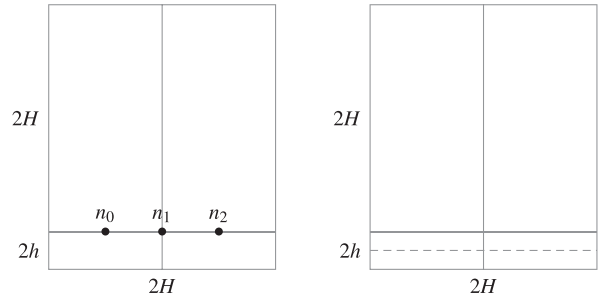

FIG. 6. Edge patches in the local coordinate system.

FIG. 7. Flat parts of edge patches.

For further use we define the following linearly independent functions:

$$\phi_0 \coloneqq \chi_M - \frac{|M|}{|M'|}\chi_{M'},$$

$$\phi_{1,M}(x,y) \coloneqq \frac{x}{H}\chi_M(x,y) \quad \text{and} \quad \phi_{2,M}(x,y) \coloneqq \left(1 - \frac{2\,|x|}{H}\right)\chi_M(x,y). \tag{5.3}$$

The pressure space $M_{\mathcal{P}}(\omega)$ is included in $\widetilde{M_{\mathcal{P}}} \coloneqq M_{\mathcal{P}}(M') \oplus M_{\mathcal{P}}(M) \oplus \operatorname{span}\{\phi_0\}$. We will prove the inf-sup condition between this larger pressure space and $\boldsymbol{V}_{\mathcal{P}}(\omega)$. As a consequence the Taylor–Hood pair will be uniformly stable on ω. As a first step, in the next result we state a decomposition of the space $M_{\mathcal{P}}(M)$.

LEMMA 5.2 Let $M = [-H, H] \times [-h, h]$ be partitioned as in Fig. 7. Then $M_{\mathcal{P}}(M)$ can be decomposed as $M_{\mathcal{P}}(M) = B_M \oplus G_M$, where

$$B_M \coloneqq \{q \in M_{\mathcal{P}}(M) \colon \partial_y q = 0 \text{ in } M\} = \operatorname{span}\{\phi_{1,M}, \phi_{2,M}\},$$

and

$$G_M \coloneqq \{q \in M_{\mathcal{P}}(M) \colon \ (q, q_s)_M = 0 \text{ for all } q_s \in B_M\}.$$

Moreover, for all $v \in H_0^1(M)$ the following holds:

$$\left(\partial_y v, q\right)_M = 0 \quad \text{for all } q \in B_M, \tag{5.4}$$

Downloaded from https://academic.oup.com/imajna/advance-article-abstract/doi/10.1093/imanum/drz028/5526934 by University of Edinburgh user on 08 December 2019

and for every $q \in G_M$ there exists $(0, w) \in \boldsymbol{V}_{\mathcal{P}}(M) \cap \boldsymbol{H}_0^1(M)$ such that

$$\left(\partial_y w, q\right)_M = \|q\|_{0,M}^2 \quad \text{and} \quad |w|_{1,M} \leq C_1 \|q\|_{0,M}, \tag{5.5}$$

where C_1 is independent of the size and shape of the elements in $\mathcal{P}$.

Proof. As it is clear from the context we will omit the subscript M in this proof. The orthogonality (5.4) follows using integration by parts. Hence, we only need to prove (5.5). We split the remainder of the proof into two cases.

Case 1: $M = [-H, H] \times [-h, h]$ is split at $x = 0$ into two anisotropic cells belonging to $\mathcal{P}$; see Fig. 7 (left). First, we extend the set $\{\phi_1, \phi_2\}$ to a basis of $M_{\mathcal{P}}(M) = \text{span}\{\phi_1, \phi_2, \phi_3, \phi_4, \phi_5\}$ where ϕ_1 and ϕ_2 are defined as in (5.3), and

$$\phi_3(x, y) := -\frac{y}{h}, \quad \phi_4 := \sqrt{3}\phi_1\phi_3 \quad \text{and} \quad \phi_5 := \sqrt{3}\phi_2\phi_3.$$

A direct computation, using Fubini's theorem and the fact that each of the functions $\{\phi_1, \phi_2, \phi_3\}$ has zero average, yields the orthogonalities

$$\left(\phi_i, \phi_j\right)_M = \delta_{ij} \left\|\phi_i\right\|_{0,M}^2 = \delta_{ij} \frac{|M|}{3} \quad \text{for } i, j \in \{1, \ldots, 5\},$$

and then $G_M = \text{span}\{\phi_3, \phi_4, \phi_5\}$, as $\phi_1, \phi_2 \in B_M$. To prove (5.5) let $g_1 \in G_M$, that is, $g_1 = \sum_{i=3}^5 q_i\phi_i$, for some real coefficients q_3, q_4, q_5, and $\left\|g_1\right\|_{0,M}^2 = \frac{1}{3}|M| \sum_{i=3}^5 q_i^2$. Let $\boldsymbol{p}_0, \boldsymbol{p}_1, \boldsymbol{p}_2 \in \mathring{M}$ be the locations of the dof of $\boldsymbol{V}_{\mathcal{P}}(\omega)$ in $\mathring{M}$ (Fig. 7, left), and let $b_0, b_1, b_2 \in H_0^1(M)$ be the piecewise $\mathbb{Q}_2$ bubble functions, such that $b_i(\boldsymbol{p}_j) = \delta_{ij}$ and $(0, b_i) \in \boldsymbol{V}_{\mathcal{P}}(\omega)$. Let, in addition, $v_3 := b_2 + b_0$, $v_4 := b_2 - b_0$ and $v_5 := b_1 - \frac{1}{4}(b_0 + b_2)$. A direct calculation using Fubini's theorem gives

$$\begin{aligned}
&\left(\partial_y v_3, \phi_3\right)_M = \frac{16H}{9}, && \left(\partial_y v_4, \phi_3\right)_M = 0, && \left(\partial_y v_5, \phi_3\right)_M = 0,\\
&\left(\partial_y v_3, \phi_4\right)_M = 0, && \left(\partial_y v_4, \phi_4\right)_M = \frac{8H}{3\sqrt{3}}, && \left(\partial_y v_5, \phi_4\right)_M = 0,\\
&\left(\partial_y v_3, \phi_5\right)_M = 0, && \left(\partial_y v_4, \phi_5\right)_M = 0, && \left(\partial_y v_5, \phi_5\right)_M = \frac{4H}{3\sqrt{3}}.
\end{aligned} \tag{5.6}$$

Hence, defining $v^\star = \alpha_3 q_3 v_3 + \alpha_4 q_4 v_4 + \alpha_5 q_5 v_5$ with $\alpha_3 = \frac{3h}{4}, \alpha_4 = \frac{\sqrt{3}h}{2}$ and $\alpha_5 = \sqrt{3}h$, we obtain

$$\left(\partial_y v^\star, g_1\right)_M = \sum_{i=3}^5 \left\|q_i\phi_i\right\|_{0,M}^2 = \left\|g_1\right\|_{0,M}^2. \tag{5.7}$$

Downloaded from https://academic.oup.com/imajna/advance-article-abstract/doi/10.1093/imanum/drz028/5526934 by University of Edinburgh user on 08 December 2019

Finally, since $|\alpha_i| \leq \sqrt{3}h$ and $|v_i|^2_{1,M} \leq \tilde{C}h^{-2}|M|/3$, we get

$$|v^\star|^2_{1,M} \leq 3\sum_{i=3}^{5} |\alpha_i q_i v_i|^2_{1,M} \leq 3\tilde{C}\sum_{i=3}^{5} q_i^2 h^2 \left(h^{-2}|M|\right) = 9\tilde{C}\sum_{i=3}^{5} \|q_i\phi_i\|^2_{0,M}, \tag{5.8}$$

which, since $(0, v^\star) \in \boldsymbol{V}_{\mathcal{P}}(M)$, finishes the first case with $C_1 = 3\sqrt{\tilde{C}}$.
Case 2: We now consider the case where $M := [-H, H] \times [-h, h]$ is divided into four rectangles $K \in \mathcal{P}$ obtained by splitting M along the lines $x = 0$ and $y = 0$, as depicted in Fig. 7 (right). We extend the set $\{\phi_1, \phi_2, \phi_3, \phi_4, \phi_5\}$, introduced in the proof of the first case, to a basis of $M_{\mathcal{P}}(M)$ by adding the following functions:

$$\phi_6(x,y) := \begin{cases} \phi_3(x, 2y-h) & \text{if } y > 0\,, \\ -\phi_3(x, 2y+h) & \text{if } y \leq 0, \end{cases} \quad \phi_7 := \sqrt{3}\phi_1\phi_6,\ \phi_8 := \sqrt{3}\phi_2\phi_6.$$

These functions are even in y, and then proceeding as before we get

$$\left(\phi_i, \phi_j\right)_M = \delta_{ij}\|\phi_i\|^2_{0,M} = \delta_{ij}\frac{|M|}{3} \quad \text{for } i,j \in \{1,\ldots,8\}.$$

Now let $\tilde{g} = g_1 + g_2 \in G_M$, where $g_1 = \sum_{i=3}^{5} q_i\phi_i$ and $g_2 = \sum_{i=6}^{8} q_i\phi_i$, for some real coefficients $q_3, \ldots, q_8$. Thanks to the definition of the function ϕ_6, we observe that g_2 can be expressed as follows:

$$g_2(x,y) = \begin{cases} (q_6\phi_3 + q_7\phi_4 + q_8\phi_5)(x, 2y-h) & \text{if } y > 0, \\ -(q_6\phi_3 + q_7\phi_4 + q_8\phi_5)(x, 2y+h) & \text{if } y \leq 0. \end{cases}$$

Then, using the function $v^\star$ from the previous case, we consider the function $\tilde{v} := v^\star + v_2^\star$, where

$$v_2^\star(x,y) := \begin{cases} \left(\alpha_6 q_6 v_3 + \alpha_7 q_7 v_4 + \alpha_8 q_8 v_5\right)(x, 2y-h) & \text{if } y > 0, \\ -\left(\alpha_6 q_6 v_3 + \alpha_7 q_7 v_4 + \alpha_8 q_8 v_5\right)(x, 2y+h) & \text{if } y \leq 0, \end{cases}$$

where $\alpha_i, i = 6, 7, 8$ are geometric constants to be determined. We note that $(0, v_2^\star) \in \boldsymbol{V}_{\mathcal{P}}(M)$.

Now we prove $\left(\partial_y(v^\star + v_2^\star), g_1 + g_2\right)_M = \|\tilde{g}\|^2_{0,M}$. To this end we recall (5.7) and since g_2 and $\partial_y v_2^\star$ are even in y, and g_1 and $\partial_y v^\star$ are odd in y, we obtain the orthogonalities

$$\left(\partial_y v_2^\star, g_1\right)_M = 0 \quad \text{and} \quad \left(\partial_y v^\star, g_2\right)_M = 0.$$

In addition, integrating by substitution and applying (5.6) gives

$$\left(\partial_y v_2^\star, g_2\right)_M = 2\int_0^h \int_{-H}^{H} \partial_y v_2^\star g_2 \,\mathrm{d}x\,\mathrm{d}y = 2\sum_{i=6}^{8} q_i^2\,\alpha_i \left(\partial_y v_{i-3}, \phi_{i-3}\right)_M,$$

Downloaded from https://academic.oup.com/imajna/advance-article-abstract/doi/10.1093/imanum/drz028/5526934 by University of Edinburgh user on 08 December 2019

which on choosing $\alpha_i := \alpha_{i-3}/2$ $(i = 6, 7, 8)$ gives

$$\left(\partial_y(v^\star + v_2^\star), \tilde{g}\right)_M = \sum_{i=3}^{5} \left\|q_i\phi_i\right\|_{0,M}^2 + \sum_{i=6}^{8} \left\|q_i\phi_{i-3}\right\|_{0,M}^2 = \|\tilde{g}\|_{0,M}^2.$$

Finally, we prove $|v|_{1,M} \leq C_1 \|q\|_{0,M}$. First, applying Cauchy's inequality and considering the scaling (w.r.t. y) inside $v_2^\star$ as well as $\alpha_i = \alpha_{i-3}/2$, we get

$$\left|v_2^\star\right|_{1,M}^2 \leq 3\left(4\sum_{i=6}^{8} \left|\alpha_i q_i v_{i-3}\right|_{1,M}^2\right) = 3\left(\sum_{i=6}^{8} q_i^2 \left|\alpha_{i-3} v_{i-3}\right|_{1,M}^2\right).$$

Now, using $\left|\alpha_i v_i\right|_{1,M}^2 \leq \tilde{C}\,|M| = 3\tilde{C}\left\|\phi_i\right\|_{0,M}^2$ (as in Case 1) we get

$$\left|v_2^\star\right|_{1,M}^2 \leq 3\tilde{C}\sum_{i=6}^{8} \left\|q_i\phi_{i-3}\right\|_{0,M}^2 = 9\tilde{C}\left\|g_2\right\|_{0,M}^2,$$

where $\tilde{C}$ is the same constant as in (5.8). Finally, recalling that $v^\star$ is even in y, and $v_2^\star$ is odd in y, we get $\left(\nabla v^\star, \nabla v_2^\star\right)_M = 0$ and arrive at

$$\begin{aligned} \left|v^\star + v_2^\star\right|_{1,M}^2 &= \left|v^\star\right|_{1,M}^2 + \left|v_2^\star\right|_{1,M}^2 \\ &\leq 9\tilde{C}\left(\left\|g_1\right\|_{0,M}^2 + \left\|g_2\right\|_{0,M}^2\right) = 9\tilde{C}\,\|\tilde{g}\|_{0,M}^2, \end{aligned} \tag{5.9}$$

which finishes the proof in this case, again with the same constant $C_1 = 3\sqrt{\tilde{C}}$. □

Now we rewrite $\widetilde{M_{\mathcal{P}}} = M_{\mathcal{P}}(M') \oplus M_{\mathcal{P}}(M) \oplus \operatorname{span}\left\{\phi_0\right\} = G_\omega \oplus B_\omega$ where

$$G_\omega := M_{\mathcal{P}}(M') \oplus G_M \quad \text{and} \quad B_\omega := B_M \oplus \operatorname{span}\left\{\phi_0\right\}, \tag{5.10}$$

with G_M and B_M defined as in Lemma 5.2. Let

$$\mathcal{X} := \boldsymbol{V}_{\mathcal{P}}(M') \oplus \left\{(0, v) \in \boldsymbol{V}_{\mathcal{P}}(M)\right\} \subset \boldsymbol{V}_{\mathcal{P}}(\omega). \tag{5.11}$$

Then, using Lemma 5.2 and the stability of the Taylor–Hood pair on M' (which is due to M' being partitioned in a shape-regular way), we conclude the uniform inf-sup condition

$$\inf_{q \in G_\omega} \sup_{\boldsymbol{v} \in \mathcal{X}} \frac{(\operatorname{div} \boldsymbol{v}, q)_\omega}{\|q\|_{0,\omega}\,|\boldsymbol{v}|_{1,\omega}} \geq \beta_2, \tag{5.12}$$

where β_2 is independent of the aspect ratio, that is, the quotient h/H. From (5.12) it follows that G_ω is controlled by a subset of $\boldsymbol{V}_{\mathcal{P}}(\omega)$ that vanishes on $\gamma := M \cap M'$. To control the remaining part of $\widetilde{M_{\mathcal{P}}}$ we need the bubble functions connecting M and M'. This is stated in the next result.

Downloaded from https://academic.oup.com/imajna/advance-article-abstract/doi/10.1093/imanum/drz028/5526934 by University of Edinburgh user on 08 December 2019

LEMMA 5.3 Let B_ω be defined as in (5.10). Then there exists a constant $\beta_1 > 0$ independent of h and H, such that

$$\sup_{\boldsymbol{v}\in \boldsymbol{V}_{\mathcal{P}}(\omega)} \frac{(\operatorname{div} \boldsymbol{v}, q)_\omega}{|\boldsymbol{v}|_{1,\omega}} \geq \beta_1 \|q\|_{0,\omega} \quad \text{for all } q \in B_\omega.$$

Proof. Let $\boldsymbol{n}_0, \boldsymbol{n}_1, \boldsymbol{n}_2 \in \gamma$ be the locations of the dof of $\boldsymbol{V}_{\mathcal{P}}(\omega)$ on γ (Fig. 6), and let $f_0, f_1, f_2 \in H^1_0(\omega)$ be the unique piecewise $\mathbb{Q}_2$ functions such that $f_i(\boldsymbol{n}_j) = \delta_{ij}$, $(0, f_i) \in \boldsymbol{V}_{\mathcal{P}}(\omega)$, and f_i are piecewise affine in y. Let $q \in B_\omega$ be arbitrary, that is, $q = q_0\phi_0 + q_1\phi_{1,M} + q_2\phi_{2,M}$ for some $q_0, q_1, q_2 \in \mathbb{R}$. Let $w^\star := \sum_{i=0}^2 \alpha_i w_i$ where α_i are coefficients to be chosen and $w_0 := f_0 + f_2$, $w_1 := f_2 - f_0$ and $w_2 := f_1 - \frac{1}{4}(f_0 + f_2)$. Using the fact that γ consists of two edges of equal lengths, a direct computation gives the orthogonalities

$$\begin{aligned} &\left(w_0, \phi_{1,M}\right)_\gamma = 0, \qquad \left(w_1, [\![\phi_0]\!]\right)_\gamma = 0, \qquad \left(w_2, [\![\phi_0]\!]\right)_\gamma = 0, \\ &\left(w_0, \phi_{2,M}\right)_\gamma = 0, \qquad \left(w_1, \phi_{2,M}\right)_\gamma = 0, \qquad \left(w_2, \phi_{1,M}\right)_\gamma = 0, \end{aligned}$$

where $[\![\phi_0]\!]$ is the jump of ϕ_0 across γ. Then integration by parts gives

$$\left(\partial_y w^\star, q\right)_\omega = \left(w^\star, [\![q]\!]\right)_\gamma = \alpha_0 q_0 \left(w_0, [\![\phi_0]\!]\right)_\gamma + \sum_{i=1}^2 \alpha_i q_i \left(w_i, \phi_{i,M}\right)_\gamma.$$

In addition

$$\begin{aligned} &\left(w_1, \phi_{1,M}\right)_\gamma = \frac{2H}{3}, \quad \left(w_2, \phi_{2,M}\right)_\gamma = \left(f_1, \phi_{2,M}\right)_\gamma = \frac{H}{3} \quad \text{and} \\ &\left(w_0, [\![\phi_0]\!]\right)_\gamma = \frac{4H}{3} [\![\phi_0]\!]_\gamma. \end{aligned}$$

Since $|M| [\![\phi_0]\!] = \|\phi_0\|^2_{0,\omega}$ and $\|\phi_{i,M}\|^2_{0,\omega} = \|\phi_i\|^2_{0,M} = (2H/3)2h$ we set $\alpha_0 := 3hq_0$, $\alpha_1 := 2hq_1$ and $\alpha_2 := 4hq_2$ to obtain

$$\left(\partial_y w^\star, q\right)_\omega = \|q\|^2_{0,\omega}.$$

Finally, since $|\alpha_i| \leq 4hq_i$ and $|w_i|^2_{1,\omega} \leq 3\sum_{j=0}^2 |f_j|^2_{1,\omega} \leq C\left(h^{-2}|M| + H^{-2}|M'|\right)$, we get

$$\begin{aligned} |w^\star|^2_{1,\omega} \leq 3\sum_{i=0}^2 |\alpha_i w_i|^2_{1,\omega} \;&\leq\; C\sum_{i=0}^2 q_i^2 h^2 \left(\frac{1}{h^2}|M| + \frac{1}{H^2}|M'|\right) \\ &\leq\; C\sum_{i=0}^2 q_i^2 |M| \left(1 + \frac{|M|}{|M'|}\right) \leq C\sum_{i=0}^2 \|q_i\phi_i\|^2_{0,\omega} =: \beta_1^{-2} \|q\|^2_{0,\omega}, \end{aligned}$$

which finishes the proof since $(0, w^\star) \in \boldsymbol{V}_{\mathcal{P}}(\omega)$. □

Downloaded from https://academic.oup.com/imajna/advance-article-abstract/doi/10.1093/imanum/drz028/5526934 by University of Edinburgh user on 08 December 2019

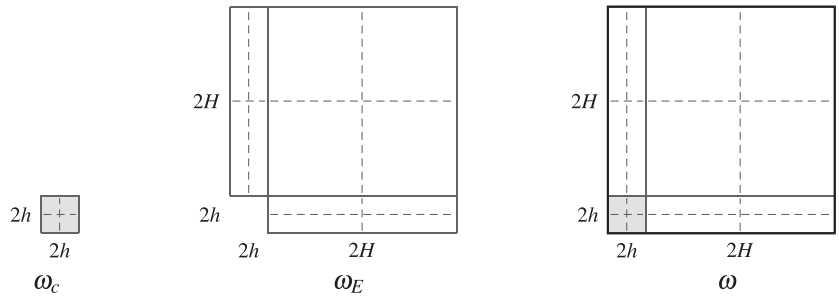

FIG. 8. A corner patch decomposed into ω_c and ω_E satisfying Hypotheses 3.4 and 3.1, respectively.

The proof of Theorem 3.2 appears then as an application of Lemma 5.1. In fact, recall the decomposition $M_{\mathcal{P}}(\omega) \subset \widetilde{M_{\mathcal{P}}} = G_\omega \oplus B_\omega$, where G_ω and B_ω are defined in (5.10). Let $q \in G_\omega \oplus B_\omega$, and recall the definition (5.11) of $\mathcal{X}$. Also, let $\Pi_B q$ be the $L^2(\omega)$ projection of q onto B_ω. Then, from (5.4) and the fact that $\Pi_B(q)$ is constant in M', we get $\left(\Pi_B q, \operatorname{div} \boldsymbol{v}\right)_\omega = 0$ for all $\boldsymbol{v} \in \mathcal{X}$. Hence,

$$\begin{aligned}\sup_{\boldsymbol{v}\in \boldsymbol{V}_{\mathcal{P}}} \frac{(q, \operatorname{div} \boldsymbol{v})_\omega}{|\boldsymbol{v}|_{1,\omega}} &\geq \sup_{\boldsymbol{v}\in \mathcal{X}} \frac{(q, \operatorname{div} \boldsymbol{v})_\omega}{|\boldsymbol{v}|_{1,\omega}} \\ &= \sup_{\boldsymbol{v}\in \mathcal{X}} \frac{\left(q - \Pi_B q, \operatorname{div} \boldsymbol{v}\right)_\omega}{|\boldsymbol{v}|_{1,\omega}} \geq \beta_2 \left\| q - \Pi_B q \right\|_{0,\omega},\end{aligned}$$

where we applied $q - \Pi_B q \in G_\omega$ and (5.12). Finally, Lemma 5.3 gives

$$\sup_{\boldsymbol{v}\in \boldsymbol{V}_{\mathcal{P}}} \frac{\left(\Pi_B q, \operatorname{div} \boldsymbol{v}\right)_\omega}{|\boldsymbol{v}|_{1,\omega}} \geq \beta_1 \left\| \Pi_B q \right\|_{0,\omega},$$

which finishes the proof upon application of Lemma 5.1 with a constant $\beta = \frac{\beta_1\beta_2}{1+\beta_1+\beta_2}$ independent of the size and aspect ratios of the edge patch.

REMARK 5.4 The essential part of the independence of the constant β (in Theorem 3.2) of the aspect ratio is given by the proof of Lemma 5.2. We observed in that proof that, for both cases, the constant C_1 is given by $3\sqrt{\widetilde{C}}$, and then it was unaffected by the additional refinement of the edge patch (see inequalities (5.8) and (5.9)). This confirms what was claimed in Remark 3.3 and is affirmed by numerical experiments.

REMARK 5.5 It is worth noticing that the proof of Theorem 3.2 provides the inf-sup stability of a family of elements that contains the lowest-order Taylor–Hood pair. In fact, the pressure space is allowed to be discontinuous across γ, which somehow generalizes the results known so far.

REMARK 5.6 A closer look at the proofs of Lemmas 5.2 and 5.3 and Theorem 3.2 shows that the technique can be applied to 'overlapped' edge patches, as shown for instance in Fig. 1(f) or Fig. 8 (center). In this case Lemma 5.2 has to be applied twice; that is, there are two flat parts, say M_1 and M_2, where M_2 contains the vertically aligned 'long and thin' cells. Then $M_{\mathcal{P}}(M_2)$ has to be decomposed into $B_{M_2} = \left\{q \in M_{\mathcal{P}}(M_2) \colon \partial_x q = 0 \text{ in } M_2\right\}$ and G_{M_2}. Hence, using the same arguments there exists $(v, 0) \in$

Downloaded from https://academic.oup.com/imajna/advance-article-abstract/doi/10.1093/imanum/drz028/5526934 by University of Edinburgh user on 08 December 2019

$\boldsymbol{V}_{\mathcal{P}}(M_2)$ such that $\left(\partial_x v, g\right)_{M_2} = \|g\|^2_{0,M_2}$ and $|v|_{1,M_2} \leq C_1 \|g\|_{0,M_2}$ for all $g \in G_{M_2}$. Then, similar to (5.10) and the arguments thereafter, the pair consisting of the velocity space $\mathcal{X} \coloneqq \left\{(0,v) \in \boldsymbol{V}_{\mathcal{P}}(M_1)\right\} \oplus \boldsymbol{V}_{\mathcal{P}}(M') \oplus \left\{(v,0) \in \boldsymbol{V}_{\mathcal{P}}(M_2)\right\}$ and the pressure space $G_\omega \coloneqq G_{M_1} \oplus M_{\mathcal{P}}(M') \oplus G_{M_2}$ is uniformly inf-sup stable. Then an adapted proof of Lemma 5.3 shows that $B_\omega = B_{M_1} \oplus B_{M_2} \oplus \operatorname{span}\left\{\phi_0, \phi_0'\right\}$, where ϕ_0' is another piecewise constant function, is controlled by the six bubbles on the edges connecting M_1, M' and M_2, M'. Finally, the proof of Theorem 3.2 follows analogously considering these modified definitions of G_ω, B_ω and $\mathcal{X}$.

5.2 Proof of Theorem 3.5

In this section we use notation $\omega_{\boldsymbol{c}}, \omega_E$, and ω as suggested in Fig. 8 for the complete and parts of the (refined) corner patch.

As done in the previous section we see that

$$M_{\mathcal{P}}(\omega) \subset \widetilde{M_{\mathcal{P}}} \coloneqq M_{\mathcal{P}}(\omega_E) \oplus M_{\mathcal{P}}(\omega_{\boldsymbol{c}}) \oplus \operatorname{span}\left\{\phi_{\boldsymbol{c}}\right\},$$

where $\phi_{\boldsymbol{c}}$ is defined as

$$\phi_{\boldsymbol{c}}(x,y) = \begin{cases} 1 & \text{if } (x,y) \in \omega_{\boldsymbol{c}}, \\ -\frac{|\omega_{\boldsymbol{c}}|}{|\omega_E|} & \text{otherwise.} \end{cases}$$

We apply the technique developed in Ainsworth *et al.* (2015) to prove Theorem 3.5. Thanks to Theorem 3.2, we know that the pair $\boldsymbol{V}_{\mathcal{P}}(\omega_E) \times M_{\mathcal{P}}(\omega_E)$ is uniformly inf-sup stable; that is, its stability constant does not depend on Hh^{-1}. In addition, if we recall Hypothesis 3.4, then the Taylor–Hood pair is inf-sup stable on $\omega_{\boldsymbol{c}}$.

Now let $q \in M_{\mathcal{P}}(\omega)$, that is, $q = q^\star + \Pi_{\boldsymbol{c}} q$, where $q^\star \in M_{\mathcal{P}}(\omega_{\boldsymbol{c}}) \oplus M_{\mathcal{P}}(\omega_E)$ and $\Pi_{\boldsymbol{c}} q \in \operatorname{span}\left\{\phi_{\boldsymbol{c}}\right\}$ is constant on $\omega_{\boldsymbol{c}}$ and ω_E. Hence, the inf-sup conditions on $\omega_{\boldsymbol{c}}$ and ω_E (mentioned above) imply

$$\sup_{\boldsymbol{v} \in \boldsymbol{V}_{\mathcal{P}}(\omega)} \frac{(q, \operatorname{div} \boldsymbol{v})_\omega}{|\boldsymbol{v}|_{1,\omega}} \geq \sup_{\boldsymbol{v} \in \boldsymbol{V}_{\mathcal{P}}(\omega_E) \oplus \boldsymbol{V}_{\mathcal{P}}(\omega_{\boldsymbol{c}})} \frac{(q^\star, \operatorname{div} \boldsymbol{v})_\omega}{|\boldsymbol{v}|_{1,\omega}} \geq \min\left\{\beta, \beta_{\boldsymbol{c}}\right\} \left\|q^\star\right\|_{0,\omega},$$

where β is from Theorem 3.2 and $\beta_{\boldsymbol{c}}$ is from Hypothesis 3.4. We will then finish the proof by showing there exists a constant $C > 0$ such that

$$\left\|q^\star\right\|_{0,\omega} \geq C \left\|\Pi_{\boldsymbol{c}} q\right\|_{0,\omega}.$$

To this end we denote by $\langle q \rangle_\omega$ the mean value of q over $\omega \subset \Omega$. Then we note that the projection $\Pi_{\boldsymbol{c}} q$ is given by

$$\Pi_{\boldsymbol{c}} q = \langle q \rangle_{\omega_{\boldsymbol{c}}} \chi_{\omega_{\boldsymbol{c}}} + \langle q \rangle_{\omega_E} \chi_{\omega_E},$$

and since $0 = \langle q \rangle_\omega$ we have $\langle q \rangle_{\omega_E} = -\left|\omega_{\boldsymbol{c}}\right| \left|\omega_E\right|^{-1} \langle q \rangle_{\omega_{\boldsymbol{c}}}$. Hence,

$$\left\|\Pi_{\boldsymbol{c}} q\right\|^2_{0,\omega} = \left|\omega_E\right| \langle q \rangle^2_{\omega_E} + \left|\omega_{\boldsymbol{c}}\right| \langle q \rangle^2_{\omega_{\boldsymbol{c}}} = \left(\frac{\left|\omega_{\boldsymbol{c}}\right|}{\left|\omega_E\right|} + 1\right) \left|\omega_{\boldsymbol{c}}\right| \langle q \rangle^2_{\omega_{\boldsymbol{c}}} = C_3 \left|\omega_{\boldsymbol{c}}\right| \langle q \rangle^2_{\omega_{\boldsymbol{c}}}, \tag{5.13}$$

Downloaded from https://academic.oup.com/imajna/advance-article-abstract/doi/10.1093/imanum/drz028/5526934 by University of Edinburgh user on 08 December 2019

where $C_3 = |\omega| \left|\omega_E\right|^{-1} \geq 1$. Now let $\Gamma_{\boldsymbol{c}} := \omega_{\boldsymbol{c}} \cap \omega_E$, and let $e \subset \Gamma_{\boldsymbol{c}}$ be an arbitrary edge satisfying $e = K_e \cap K_e'$ with $K_e \subset \omega_{\boldsymbol{c}}$. Then, from $\langle q \rangle_{\omega_{\boldsymbol{c}}} - \langle q \rangle_{\omega_E} = \left\langle [\![\Pi_{\boldsymbol{c}} q]\!] \right\rangle_e$, and since q is continuous in ω, we get

$$C_3 \langle q \rangle_{\omega_{\boldsymbol{c}}} = \left\langle [\![\Pi_{\boldsymbol{c}} q]\!] \right\rangle_e = - \left\langle [\![q^\star]\!] \right\rangle_e \quad \text{and} \quad \langle q \rangle_{\omega_{\boldsymbol{c}}}^2 = C_3^{-2} \left\langle [\![q^\star]\!] \right\rangle_e^2.$$

Then Cauchy's inequality and Ainsworth *et al.* (2015, Lemma 2.1) yield

$$\begin{aligned}
\langle q \rangle_{\omega_{\boldsymbol{c}}}^2 &= \frac{1}{|\Gamma_{\boldsymbol{c}}|} \int_{\Gamma_{\boldsymbol{c}}} \langle q \rangle_{\omega_{\boldsymbol{c}}}^2 \\
&= \frac{1}{C_3^2 |\Gamma_{\boldsymbol{c}}|} \sum_{e \subset \Gamma_{\boldsymbol{c}}} \int_e \left\langle [\![q^\star]\!] \right\rangle_e^2 \\
&\leq \frac{1}{C_3^2 |\Gamma_{\boldsymbol{c}}|} \sum_{e \subset \Gamma_{\boldsymbol{c}}} \int_e \frac{1}{|e|} \left\| [\![q^\star]\!] \right\|_{0,e}^2 \\
&\leq \frac{1}{C_3^2} \sum_{e \subset \Gamma_{\boldsymbol{c}}} \frac{|e|}{|\Gamma_{\boldsymbol{c}}|} \left(\frac{1}{|K_e|} + \frac{1}{|K_e'|} \right) 4 \left\| q^\star \right\|_{0, K_e \cup K_e'}^2.
\end{aligned}$$

Now using $|K_e| \leq |K_e'|$, $\frac{|e|}{|\Gamma_{\boldsymbol{c}}|} \frac{|\omega_{\boldsymbol{c}}|}{|K_e|} = 1$ and $1/C_3 \leq 1$ we get from (5.13),

$$\left\| \Pi_{\boldsymbol{c}} q \right\|_{0,\omega}^2 = C_3 |\omega_{\boldsymbol{c}}| \langle q \rangle_{\omega_{\boldsymbol{c}}}^2 \leq \frac{1}{C_3} \sum_{e \subset \Gamma_{\boldsymbol{c}}} \frac{|e|}{|\Gamma_{\boldsymbol{c}}|} \frac{|\omega_{\boldsymbol{c}}|}{|K_e|} 8 \left\| q^\star \right\|_{0, K_e \cup K_e'}^2 \leq 8 \left\| q^\star \right\|_{0,\omega}^2,$$

as required.

REMARK 5.7 In this proof we have not considered the possibility of refining the corner patches. If we were to consider that case then in the last step of the above proof we would be led to use the fact that, for a corner patch that has been refined uniformly r times, we have

$$\frac{|e|}{|\Gamma_{\boldsymbol{c}}|} \frac{|\omega_{\boldsymbol{c}}|}{|K_e|} = 2^{r-1}.$$

This would give as a result the inf-sup constant

$$\beta_{\mathfrak{P}} \sim C 2^{-\frac{r-1}{2}},$$

which shows a dependency of the inf-sup constants on the refinement of the partition. This dependency is not an artifact of the proof, as the numerical results in Table 4 show.

6. The triangulated case

In this section we prove Theorems 3.2 and 3.5 for triangulated edge and corner patches. A single change is required to prove Theorem 3.5, that is, we have to replace the used discrete trace estimate by one that is valid on anisotropic triangles; see, for example, Warburton & Hesthaven (2003, Theorem 3).

Then it remains to prove Theorem 3.2. To this end we note that the proofs of Lemmas 5.1 and 5.3 remain valid and we only need to prove Lemma 5.2 for triangulated anisotropic (flat) macro elements.

Downloaded from https://academic.oup.com/imajna/advance-article-abstract/doi/10.1093/imanum/drz028/5526934 by University of Edinburgh user on 08 December 2019

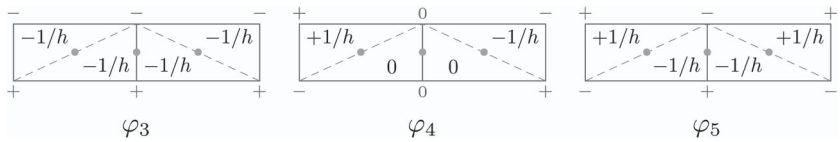

FIG. 9. Basis of G_M with sign patterns of φ_i and $\partial_y \varphi_i$.

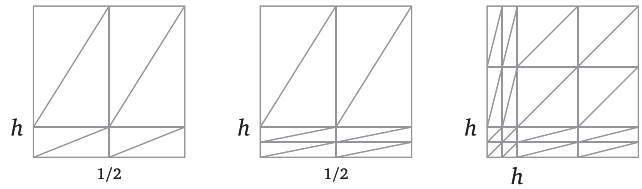

FIG. 10. Triangulated edge and corner patches satisfying the hypotheses of Theorems 3.2 and 3.5. In all cases, $\Omega = (0,1)^2$.

6.1 Proof of Theorem 3.2

We perform a direct computation that is simplified by using the following three-point quadrature formula:

$$\int_K f \,\mathrm{d}\boldsymbol{x} \approx \frac{|K|}{3} \sum_{i=1}^{3} f(\boldsymbol{m}_i),$$

where $\boldsymbol{m}_i$ are the midpoints of the edges of triangle K. This formula is exact for $f \in \mathbb{P}_2(K)$.

Now we let $M = [-H, H] \times [-h, h]$ and notice that however we triangulate M, the space $B_M = \operatorname{span}\{\phi_1, \phi_2\}$ defined in Lemma 5.2 is a subspace of $M_{\mathcal{P}}(M)$. Next we prove (5.5) on the triangulated macro element.

Case 1: M is split at $x = 0$ and then triangulated. Again we have $\dim G_M = 3$ and for a basis of G_M we choose $\{\varphi_i\}_{i=3}^5$ to be the nodal interpolants of $\{\phi_i\}_{i=3}^5$ in Lemma 5.2. These functions take the values $+1/-1/0$ at the signs $+/-/0$ shown in Fig. 9. For simplicity (but without loss of generality) we chose a triangulation on which φ_3 and φ_5 remain even in x, while φ_4 is odd in x. Additionally, the product $\varphi_3\varphi_5$ vanishes in each of the quadrature points, and therefore $\{\varphi_i\}_i$ is an orthogonal basis of G_M. Hence, for $g \in G_M$ with $g = \sum_{i=3}^5 q_i \varphi_i$, the quadrature formula yields

$$\|g\|_{0,M}^2 = \sum_{i=3}^{5} \|q_i \varphi_i\|_{0,M}^2 = \frac{|M|}{6} \left(2q_3^2 + q_4^2 + 2q_5^2\right).$$

Now, let b_0, b_1 and b_2 be the quadratic bubble functions, each supported on two triangles and taking the value 1 at the midpoint of the shared edge. Then defining v_3, v_4 and v_5 similarly to Lemma 5.2 by $v_3 := b_2 + b_0$, $v_4 := b_2 - b_0$ and $v_5 := 2b_1 - (b_2 + b_0)$ we get

$$\left(\partial_y v_i, g\right)_M = -\left(v_i, \partial_y g\right)_M = -q_i \left(v_i, \partial_y \varphi_i\right)_M \quad \text{for} \quad i = 3, 4, 5,$$

Downloaded from https://academic.oup.com/imajna/advance-article-abstract/doi/10.1093/imanum/drz028/5526934 by University of Edinburgh user on 08 December 2019

TABLE 5 *Discrete inf-sup constants of the $\mathbb{P}_2^2 \times \mathbb{P}_1$ pair on the partitions shown in Fig. 10*

h	Fig. 10 (left)	Fig. 10 (center)	Fig. 10 (right)
10^{-1}	0.3346	0.3332	0.3844
10^{-2}	0.2690	0.2677	0.3744
10^{-3}	0.2480	0.2478	0.3519
10^{-4}	0.2453	0.2452	0.3493
10^{-5}	0.2450	0.2450	0.3491

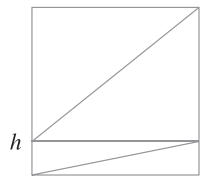

h	$\beta_{\mathcal{P}}$
10^{-1}	$1.788 \cdot 10^{-1}$
10^{-2}	$8.236 \cdot 10^{-2}$
10^{-3}	$2.725 \cdot 10^{-2}$
10^{-4}	$8.656 \cdot 10^{-3}$
10^{-5}	$2.739 \cdot 10^{-3}$

FIG. 11. A triangulated edge patch that does not satisfy Hypothesis 3.1 and the associated discrete inf-sup constants for the $\mathbb{P}_2 \times \mathbb{P}_1$ pair.

and then $v^\star := \sum_{i=3}^{5} \alpha_i v_i$ satisfies

$$\left(\partial_y v^\star, g\right)_M = -\left(v^\star, \partial_y g\right)_M = -\sum_{i=3}^{5} \alpha_i q_i \left(v_i, \partial_y \varphi_i\right)_M.$$

To calculate these products we use the quadrature formula and the values of $(\partial_y \varphi_i) i\Big|_K$, given inside the triangles shown in Fig. 9. We obtain

$$\left(v_3, \partial_y \varphi_3\right)_M = -|M|/(3h),$$
$$\left(v_4, \partial_y \varphi_4\right)_M = -|M|/(6h),$$
$$\left(v_5, \partial_y \varphi_5\right)_M = \left(2b_1, \partial_y \varphi_5\right)_M = -|M|/(3h),$$

and choosing $\alpha_i = -q_i h$ we obtain

$$\left(\partial_y v^\star, g\right)_M = \sum_{i=3}^{5} \left\| q_i \varphi_i \right\|_{0,M}^2 = \|g\|_{0,M}^2.$$

Finally, since $|\alpha_i| \leq h q_i$ and $|v_i|_{1,M}^2 \leq C h^{-2} |M|$ we get

$$|v^\star|_{1,M}^2 \leq C \sum_{i=3}^{5} |\alpha_i v_i|_{1,M}^2 \leq C \sum_{i=3}^{5} h^2 q_i^2 (h^{-2} |M|) = C \|g\|_{0,M}^2,$$

which finishes Case 1 as $(0, v^\star) \in \boldsymbol{V}_{\mathcal{P}}(M)$.

Downloaded from https://academic.oup.com/imajna/advance-article-abstract/doi/10.1093/imanum/drz028/5526934 by University of Edinburgh user on 08 December 2019

Case 2: On appropriate triangulations of a 2-by-2 macro element one can construct orthogonal bases of the velocity and pressure spaces, again even and odd in y, respectively. Then the proof follows in a similar way to Case 1.

6.2 *A numerical confirmation*

The results presented in Table 5 show that the Taylor–Hood pair is also uniformly stable on triangulated edge and corner patches. Furthermore, we see that the difference between the inf-sup constants in columns 1 and 2 is marginal, that is, the additional refinement does not affect the inf-sup constant. On the other hand, we show that Hypothesis 3.1 for edge patches must be satisfied for their triangulated versions, as Fig. 11 confirms.

7. Possible extensions

In this work we have proven the uniform inf-sup stability of the lowest-order Taylor–Hood pair in a family of anisotropic meshes. To the best of our knowledge this is the first proof available for this pair on anisotropic meshes. The numerical evidence shown suggests that the hypotheses made for the partitions (macro elements) are minimal, so the results presented here are optimal.

There are, nevertheless, open questions. The first is the possible extension to higher-order polynomials. Another possible extension is the possibility to allow geometric refinements towards a corner of a given partition. The proof of Theorem 3.5 would not fail in this situation provided the result on geometric edge patches holds. In fact, a dependency on a level of refinement as documented in Remark 5.7 would not occur. Another important open question is the validity of our result in the case of meshes that do not have an underlying structure and the case of non-affine quadrilaterals. Finally, the problem of stability of an anisotropic refinement strategy, driven by *a posteriori* error estimators, is also a topic of interest. All these constitute open questions that will be subjects of future research.

Acknowledgements

AW gratefully acknowledges the financial support given by the Asociación Mexicana de Cultura A.C. Furthermore, we are grateful to the referees for their interesting comments and suggestions.

Funding

Leverhulme Trust (RPG-2012-483).

References

Acosta, G. & Durán, R. G. (1999) The maximum angle condition for mixed and nonconforming elements: application to the Stokes equations. *SIAM J. Numer. Anal.*, **37**, 18–36 (electronic).

Ainsworth, M., Barrenechea, G. R. & Wachtel, A. (2015) Stabilization of high aspect ratio mixed finite elements for incompressible flow. *SIAM J. Numer. Anal.*, **53**, 1107–1120.

Ainsworth, M. & Coggins, P. (2000) The stability of mixed *hp*-finite element methods for Stokes flow on high aspect ratio elements. *SIAM J. Numer. Anal.*, **38**, 1721–1761 (electronic).

Apel, T., Nicaise, S. & Schöberl, J. (2001) Crouzeix–Raviart type finite elements on anisotropic meshes. *Numer. Math.*, **89**, 193–223.

Apel, T. & Randrianarivony, M. H. (2003) Stability of discretizations of the Stokes problem on anisotropic meshes. *Math. Comput. Simulation*, **61**, 437–447.

Downloaded from https://academic.oup.com/imajna/advance-article-abstract/doi/10.1093/imanum/drz028/5526934 by University of Edinburgh user on 08 December 2019

Bercovier, M. & Pironneau, O. (1979) Error estimates for finite element method solution of the Stokes problem in the primitive variables. *Numer. Math.*, **33**, 211–224.

Boffi, D. (1994) Stability of higher order triangular Hood–Taylor methods for the stationary Stokes equations. *Math. Models Methods Appl. Sci.*, **4**, 223–235.

Boffi, D. (1997) Three-dimensional finite element methods for the Stokes problem. *SIAM J. Numer. Anal.*, **34**, 664–670.

Boffi, D., Brezzi, F. & Fortin, M. (2013) *Mixed Finite Element Methods and Applications*. Springer Series in Computational Mathematics, vol. 44. Heidelberg: Springer, pp. xiv+685.

Braack, M., Lube, G. & Röhe, L. (2012) Divergence preserving interpolation on anisotropic quadrilateral meshes. *Comput. Methods Appl. Math.*, **12**, 123–138.

Brezzi, F. & Falk, R. S. (1991) Stability of higher-order Hood–Taylor methods. *SIAM J. Numer. Anal.*, **28**, 581–590.

Chen, L. (2014) A simple construction of a Fortin operator for the two dimensional Taylor–Hood element. *Comput. Math. Appl.*, **68**, 1368–1373.

Durán, R. G. (2008) Mixed finite element methods. *Mixed Finite Elements, Compatibility Conditions, and Applications*, lectures given at the C.I.M.E. Summer School held in Cetraro, 26 June–1 July 2006 (Boffi, D. & Gastaldi L. eds). Berlin; Fondazione C.I.M.E. Florence: Springer, pp. 1–44.

Durán, R. G. & Lombardi, A. L. (2008) Error estimates for the Raviart–Thomas interpolation under the maximum angle condition. *SIAM J. Numer. Anal.*, **46**, 1442–1453.

Falk, R. (2008) A Fortin operator for two-dimensional Taylor–Hood elements. *ESAIM Math. Model. Numer. Anal.*, **42**, 411–424.

Girault, V. & Raviart, P.-A. (1986) *Finite Element Methods for Navier Stokes Equations*. Berlin: Springer.

John, V. (2016) *Finite Element Methods for Incompressible Flow Problems*. Berlin: Springer.

Mardal, K., Schöberl, J. & Winther, R. (2013) A uniformly stable Fortin operator for the Taylor–Hood element. *Numer. Math.*, **123**, 537–551.

Schötzau, D. & Schwab, C. (1998) Mixed *hp*-FEM on anisotropic meshes. *Math. Models Methods Appl. Sci.*, **8**, 787–820.

Schötzau, D., Schwab, C. & Stenberg, R. (1999) Mixed *hp*-FEM on anisotropic meshes. II. Hanging nodes and tensor products of boundary layer meshes. *Numer. Math.*, **83**, 667–697.

Stenberg, R. (1990) Error analysis of some finite element methods for the Stokes problem. *Math. Comp.*, **54**, 495–508.

Taylor, C. & Hood, P. (1973) A numerical solution of the Navier–Stokes equations using the finite element technique. *Comput. & Fluids*, **1**, 73–100.

Verfürth, R. (1984) Error estimates for a mixed finite element approximation of the Stokes equations. *RAIRO Anal. Numér.*, **18**, 175–182.

Warburton, T. & Hesthaven, J. S. (2003) On the constants in *hp*-finite element trace inverse inequalities. *Comput. Methods Appl. Mech. Engrg.*, **192**, 2765–2773.

Downloaded from https://academic.oup.com/imajna/advance-article-abstract/doi/10.1093/imanum/drz028/5526934 by University of Edinburgh user on 08 December 2019